RESEARCH ARTICLE

High fill factor over 82% enabled by a biguanide doping electron transporting layer in planar perovskite solar cells

Ru GE, Fei QIN, Lin HU, Sixing XIONG, Yinhua ZHOU (✉)

Wuhan National Laboratory for Optoelectronics, School of Optical and Electronic Information, Huazhong University of Science and Technology, Wuhan 430074, China

Abstract   N-type doping in electron transport materials is an effective way to improve the electron collection and enhance the performance of the perovskite solar cells (PSCs). Here, for the first time, an antibiotic and antimicrobial compound of 1-(o-Tolyl) biguanide (oTb) is used to dope the electron transport material of phenyl-C_{61}-butyric acid methyl ester (PCBM). The oTb doping into the PCBM can increase the conductivity and reduce the work function of the PCBM. The oTb doping can significantly enhance the fill factor (FF) of the perovskite solar cells with the structure of glass/ITO/NiO$_x$/MAPbI$_3$/ (oTb)PCBM/(PEIE)/Ag. For the cells without PEIE (polyethylenimine ethoxylated) coating, the oTb doping increases the FF from 0.57 to 0.73. S-shaped of the current density-voltage (J-V) characteristic under illumination is removed after the oTb doping. For the cells with PEIE coating between the (oTb)PCBM and Ag, the oTb doping increases the FF from 0.70 to 0.82. These results show the potential of the oTb as an n-dopant in the applications of perovskite solar cells.

Keywords   perovskite solar cells, n-doping, biguanide, fill factor (FF), electron transporting layer

1   Introduction

Perovskite solar cells have been attracting extensive attention in both academia and industry due to their rapidly growth in the power conversion efficiency (PCE) [1], along with their advantages in cost, weight, manufacturing, flexibility and color tenability [2–6]. Planar inverted "p-i-n" architecture has been widely studied [7],

owing to their potential in easy fabrication, device flexibility and possibility of fabricating multi-junction cells [8–10]. The interface between electron transporting layer (ETL) and top metal electrode plays a critical role in high-performance perovskite solar cells. Fullerene or its derivatives have been generally used as the electron transporting layer in the p-i-n planar architecture [11,12]. A commonly used derivative is phenyl-C_{61}-butyric acid methyl ester (PCBM) [13,14]. The direct contact between the PCBM and metal electrode Ag is not favorable for electron transport [15,16]. Typically, an S-shape can be observed in the current density-voltage (J-V) characteristics of cells under illumination, thus resulting in the poor device performance (particularly low fill factor (FF)) [14,17]. One effective solution is to insert a separate layer, such as polyethylenimine ethoxylated (PEIE) [18] and bathocuproine (BCP) [19], between PCBM and Ag to enhance the contact and therefore improve the electron extraction. The insertion of the separate layer increases the complexity of the device fabrication. In addition, the processing solvent for this layer has to be very careful since the organic-inorganic halide perovskite films are very sensitive the polar solvents [20–22]. Another strategy is to adopt a dopant in fullerene derivatives [12,23,24]. The doping can simultaneously enhance the conductivity and shift the work function of the electron transporting layer, and therefore improve the contact between the fullerene and the metal electrode [15,17,25–27]. This strategy is technically simple and effective. However, the effective, low-cost and air-stable n-dopants are still fewly reported in the literature. The search of the such n-dopants is still going on for the community.

Here, for the first time, an antibiotic and antimicrobial compound of 1-(o-Tolyl) biguanide (oTb) is used to dope the PCBM and demonstrate the effectiveness as the electron transporting layer in the inverted perovskite solar cells. The oTb doping can increase the conductivity and lower work function of PCBM. Very impressively,

when the oTb doped PCBM films used the electron transporting layer, the FF of planar perovskite solar cells (glass/ITO/NiO$_x$/MAPbI$_3$/(oTb)PCBM/Ag) is significantly enhanced from 0.57 to 0.73, S-shape in the J-V characteristics under illumination is removed after the oTb doping. For the cells with PEIE coating between the (oTb) PCBM and Ag, the oTb doping increases the FF from 0.70 to 0.82.

2   Experimental section

2.1   Materials

1-(*o*-Tolyl) biguanide (oTb), and polyethylenimine ethoxylated (PEIE) were purchased from Sigma-Aldrich. Nickel acetate tetrahydrate Ni(CH$_3$COO)$_2$·4H$_2$O from Alfa Aesar, monoethanolamine and methoxyethanol from Sigma-Aldrich were prepared for NiO$_x$ precursor solutions. The NiO$_x$ precursor contained 0.3 g Ni (CH$_3$COO)$_2$·4H$_2$O and 0.1 g monoethanolamine in 10 g methoxyethanol. Methylamine iodide (MAI), PbI$_2$ for perovskite precursor and PCBM ($>$99%) were purchased from Xi'an Polymer Light Technology Corp.

2.2   Device fabrication

The indium tin oxide (ITO)-coated glass (CSG Holding Co. Ltd., Shenzhen) substrates process a sheet resistance of 10 Ω. The ITO glass was cleaned in sequential ultrasonic baths of detergent in deionized water, deionized water, acetone and 2-propanol for 20 min. NiO$_x$ precursor solutions were spin-coated on cleaned ITO, following an annealing at 200°C for 10 min and 400°C for 20 min. After that, the ITO/NiO$_x$ films were treated by air-plasma for 3 min and transferred to N$_2$-filled glovebox. Then, the perovskite layer was deposited on NiO$_x$ films. The precursor solution (1.3 mol MAI: 1.3 mol PbI$_2$ in GBL: DMSO = 7:3) was spin-coated by a consecutive two-step spin-coating process at 1000 r/min for 10 s, and 4000 r/min for 20 s. The anti-solvent toluene (approximately 200 μL) was quickly dropped onto the center of the films with a delay time of 28 s after the beginning of the spin-coating. Then, the substrate was annealed on a hot plate at 100°C for 10 min. PCBM solutions (20 mg/mL in chlorobenzene) with different doping ratio by oTb were fabricated on the perovskite layer at a speed of 2000 r/min. PEIE (0.1 wt.%) was spin-coated on the films to form an around 5-nm-thick interface-decorating layer. Finally, 100-nm-thick silver electrode was deposited on top of PEIE with the pressure of 5 × 10^{-7} Torr using a thermal evaporator (Mini-spectros, Kurt J. Lesker)

2.3   Film and device characterization

The thicknesses of films were measured through a surface profiler (Dektak XT, Bruker Corp). Work function of PCBM and doped PCBM were conducted by Kelvin Probe (KP020). The J-V characteristics of all devices were measured by a Keithley 2400 source-measure unit inside a N$_2$-fillerd glove box under illumination of one sun. Time-resolved photoluminescence were measured using a Delta Flex Fluorescence Lifetime System monitored at 750 nm.

3   Results and discussion

Figure 1 shows the chemical structure of the oTb and the PCBM. Biguanides are often used as drugs for diabetes mellitus, prediabetes or malaria. The oTb generally act as an antibiotic and antimicrobial compound [28]. Here, we introduce this compound into the field of solution-processed electronics. The biguanide group in oTb has the electron-donating property, which may have the doping effect like amidine [25]. In addition, the tolyl group in oTb makes the compound more soluble in organic solvents, and more compatible with PCBM. The n-doping can be achieved by mixing, which reduces the complexity and cost of manufacturing. The doping effect is demonstrated by the performance of the perovskite solar cells with the structure of ITO/NiO$_x$/MAPbI$_3$/(oTb)PCBM/Ag, as shown in Fig. 1. It is an inverted perovskite solar cell structure, with perovskite MAPbI$_3$ (CH$_3$NH$_3$PbI$_3$) as the active layer to absorb the incident photons. (oTb)PCBM represents the pristine or oTb-doped PCBM films with various doping concentrations as the electron transporting layer. Furthermore, we also fabricated perovskite solar cells with the structure of ITO/NiO$_x$/MAPbI$_3$/(oTb)PCBM/PEIE/Ag, where PEIE is inserted between the electron transporting layer and the Ag metal electrode to further enhance the electron collections of the devices [29].

The doping concentrations of 0.1, 0.3, 0.5 and 1 wt.% are studied, relative to the weight of PCBM. The (oTb) PCBM films were fabricated by spin-coating chlorobenzene solutions consisting of 20 mg/mL PCBM and oTb dopants. To understand the effect of the doping, we evaluated the conductivity of the (oTb)PCBM films on the insulated glass substrates with transmission line method (TLM) to avoid the influence of contact resistance. The device structure of TLM measurement is shown in Fig. 2 (a). The conductive channels are the silver electrodes created by the vapor deposition, with the channel width (a) of 1 mm and the length (l) of 0.1 mm (L), 0.2 mm ($2L$), 0.3 mm ($3L$) and 0.4 mm ($4L$), respectively. By measuring the I-V curves of the two adjacent silver electrodes with the length of nL (n = 1, 2, 3, 4), we can obtain the resistance (R_{nL}), which consists of intrinsic resistance and contact resistance. The R_{nL}-n curve is then drawn with n as the x-axis, which slope is the resistance (R) corresponding to the channel of length L. Using this TLM method, we can obtain a conductivity by the following equation PSCs [30]:

$$\sigma = \frac{L}{R \times d \times a},$$

where d denotes the film thickness measured by a surface profiler. The conductivity of the pristine PCBM film is about 7.44×10^{-7} S/cm. As the oTb-doping concentration increases, the conductivity of the film increases slightly, reaching 2.11×10^{-6} S/cm (1 wt.%). The increase in film conductivity indicates the doping effect of the oTb addition. Figure 2(b) also shows the work function (WF) of the films, which were fabricated on ITO glass substrates. The WF of PCBM decreases from 4.55 to 4.47 eV upon addition of 1 wt.% oTb. We conclude that the addition of oTb shifts the WF of PCBM upper which is beneficial to the electron collection by the Ag electrode.

J-V characteristics in Fig. 3(a) show the performance of the devices under AM 1.5 G conditions (100 mW/cm^2) with a structure of glass/ITO/NiO$_x$/MAPbI$_3$/(oTb)PCBM/Ag. There is an "S-shape" in the J-V characteristic under illumination of the control device with a pristine PCBM electron transporting layer, due to the poor electrical contact between the PCBM and Ag. The "S-shape" in the J-V curves gradually removes with the increase of the oTb concentration, showing an improved electron extraction

property. Table 1 summarizes the photovoltaic parameters of these devices. We can see that the open-circuit voltage (V_{OC}) values of the doped devices are higher than that of the control device (1.03 V). The short-circuit current density (J_{SC}) of the 0.1 wt.% oTb-doped device is 20.64 mA/cm^2, higher than that of the pristine PCBM, but it decreases as the concentration further increases. The most changed parameter of the photovoltaic properties is the FF, which increases from 0.57 (pristine PCBM) to 0.73 (1 wt.% oTb-doped). Figure 3(b) represents the statistical date of ten devices fabricated with pristine and doped PCBM electron transporting layer at various oTb concentrations, respectively. The average FF values of oTb-doped devices are much higher than that of pristine PCBM-based one. It increases with the increasing oTb concentration, resulting in the enhancement of the PCE. With the tradeoff of FF and J_{SC}, when the oTb doing concentration is 0.1 wt.%, the perovskite solar cell (glass/ITO/NiO$_x$/MAPbI$_3$/(oTb)PCBM/Ag) delivers a maximum PCE of 14.73%.

For comparison and further optimization of the solar cells, cells with the structure of glass/ITO/NiO$_x$/MAPbI$_3$/(oTb)PCBM/PEIE/Ag are also fabricated. A PEIE layer is inserted between the (oTb)PCBM and Ag electrode. The PEIE coating is used to further enhance the electron
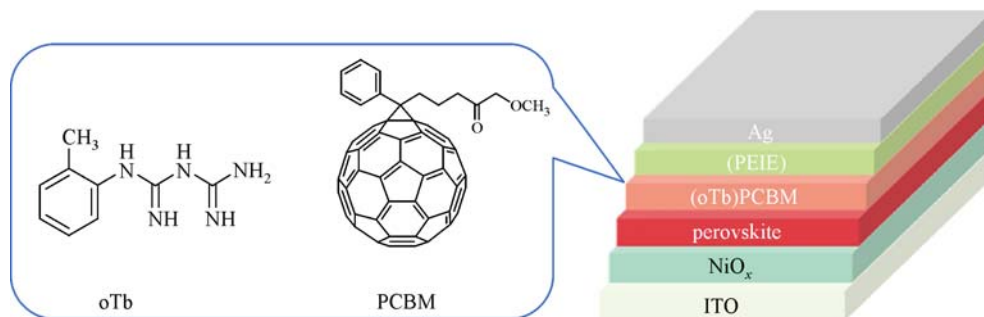

Fig. 1 Chemical structure of oTb and PCBM, and device structure of planar perovskite solar cells with the pristine or oTB doped PCBM as the electron transporting layer. Devices with and without PEIE layer between the (oTb)PCBM layer and Ag electrode are both fabricated for comparison
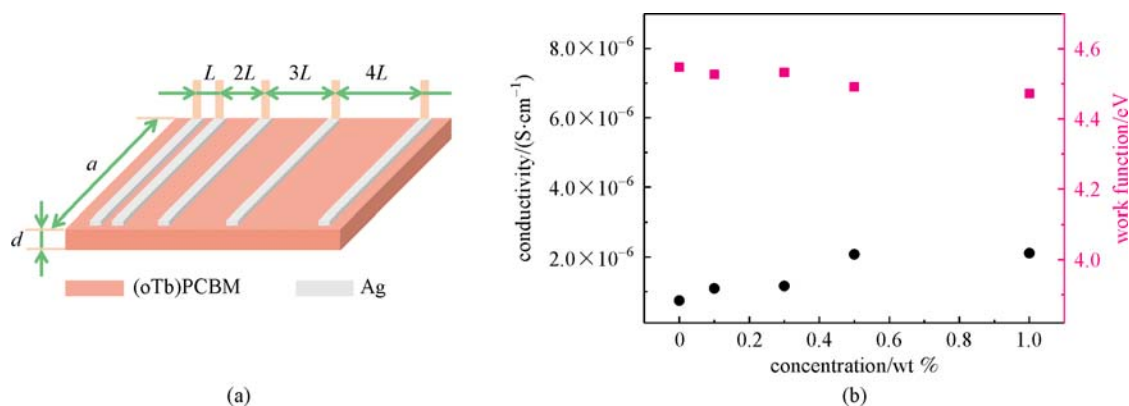

Fig. 2 (a) Device structure of the conductivity measurements (transmission line method) for the samples of (oTb)PCBM; (b) conductivities and work functions of pristine and oTb-doped PCBM films with different doping concentrations

extraction [31]. The *J-V* characteristics of the cells with different concentration of oTb doping are shown in Fig. 4. Their photovoltaic parameters are summarized in Table 2. Comparing with the cells without PEIE coating, these cells with PEIE shows higher performance. There is no "S-shape" in the *J-V* curves under illumination. For the pristine PCBM-based cell, it displays a V_{OC} of 1.06 V, J_{SC} of 20.55 mA/cm^2 and FF of 0.70. This confirms the positive effect of the PEIE role for electron extraction. The oTb doping into the PCBM electron transporting layer can

Table 1 Photovoltaic performance of the perovskite solar cells with the device structure of ITO/NiO$_x$/MAPbI$_3$/(oTb)PCBM/Ag. Note: there is no PEIE coating between the (oTb)PCBM and Ag electrode

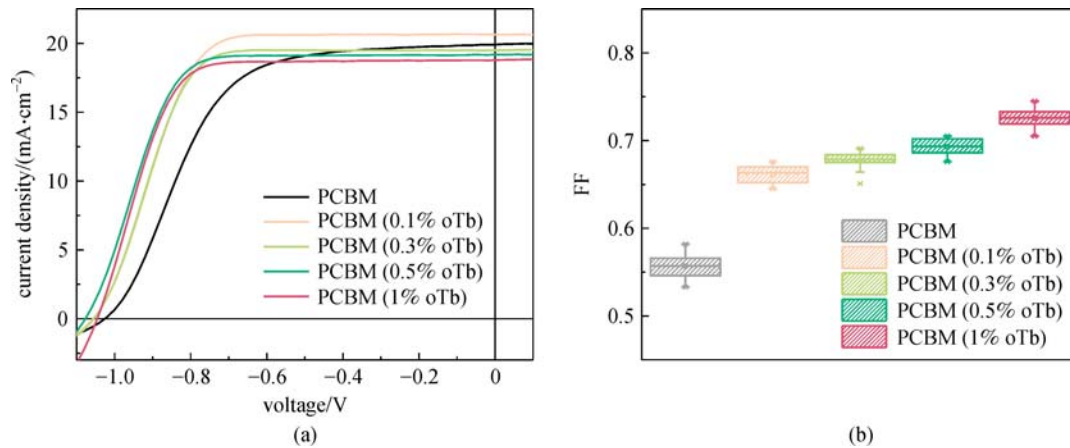| doping concentration of oTb into PCBM	V_{OC}/V	J_{SC}/(mA·cm^{-2})	FF/%	PCE/%
pristine PCBM	1.03	20.0	0.57	11.7
0.1 wt.% oTb	1.06	20.64	0.68	14.7
0.3 wt.% oTb	1.06	19.50	0.69	14.2
0.5 wt.% oTb	1.08	19.19	0.71	14.6
1 wt.% oTb	1.05	18.73	0.73	14.2

Fig. 3 (a) *J-V* curves of the planar perovskite solar cells; (b) FF standard box plots of the perovskite solar cells with the structure of ITO/NiO$_x$/MAPbI$_3$/(oTb)PCBM/Ag, where the (oTb)PCBM denotes pristien or oTb-doped PCBM films with different doping concentrations
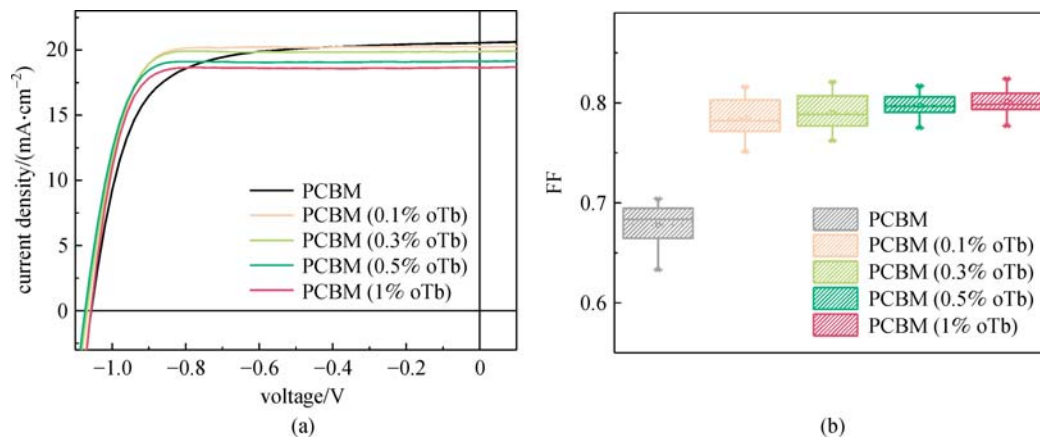

Fig. 4 (a) *J-V* curves of the planar perovskite solar cells (PSCs); (b) FF standard box plots of the PSCs with the structure of ITO/NiO$_x$/MAPbI$_3$/(oTb)PCBM/PEIE/Ag, where the (oTb)PCBM denotes pristien or oTb-doped PCBM films with different doping concentrations, and a PEIE layer is inserted between the (oTb)PCBM and Ag electrode

Table 2 Photovoltaic performance of the perovskite solar cells with the device structure of ITO/NiO$_x$/MAPbI$_3$/(oTb)PCBM/PEIE/Ag. A PEIE coating is inserted between the (oTb)PCBM and Ag electrode

doping concentration of oTb into PCBM	V_{OC}/V	J_{SC}/(mA·cm^{-2})	FF/%	PCE/%
pristine PCBM	1.06	20.55	0.70	15.1
0.1 wt.% oTb	1.06	20.25	0.80	17.1
0.3 wt.% oTb	1.07	19.89	0.80	17.1
0.5 wt.% oTb	1.07	19.13	0.81	16.6
1 wt.% oTb	1.06	18.65	0.82	16.1

further enhance the solar cell performance. The V_{OC} and J_{SC} do not increase as the doping concentration increases. Again, the oTb doping can significantly enhance the FF of the cells. Statistical FF values of 20 devices for each doping concentrations are shown in Fig. 4(b). When the oTb doping is 0.1 wt.% relative to the PCBM, FF of the cells increases to over 0.8 from 0.7 (cells with pristine PCBM). The FF reaches 0.82 when the doping concentration is 1 wt.%. Such high FF is rarely reported in the literature. The high FF confirms the potential of the oTb doping into the electron transporting layers. It should be noted that after adding PEIE layer, the FF of devices with different oTb doping ratios does not increases as much as the devices without PEIE. This is because the PEIE also improves the electron collection. The devices with PEIE (no oTb) can provide a FF of 0.70. The FF can be further enhanced to 0.82 after oTb doping. When the oTb doping concentration is 0.1 wt.%, the perovskite solar cells with the PEIE coating delivers the highest PCE of 17.13%. Time-resolved photoluminescence (PL) decay of the samples [glass/MAPbI$_3$/(oTb)PCBM] are shown in Fig. 5. When the oTb doping ratio increases, the decay time of the samples becomes longer. The prolonged lifetime might be associated with trap passivation on the surface of perovskite films [22].
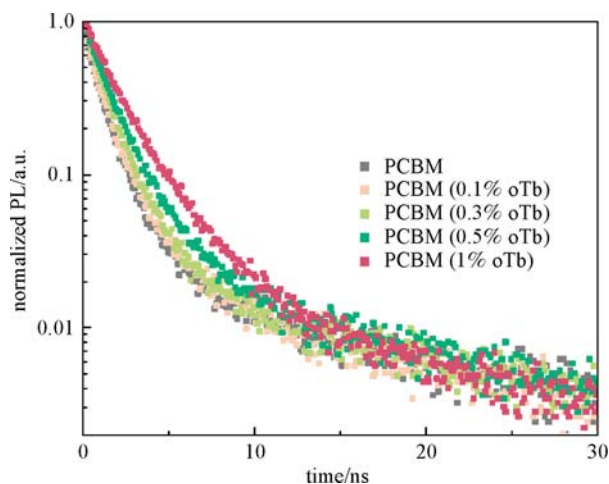
4 Conclusions

In this work, we demonstrate that an antibiotic and antimicrobial compound of 1-(o-Tolyl) biguanide (oTb) can be used as a dopant into PCBM for solution processed electronics. The addition of oTb can increase the conductivity and reduce the work function of the PCBM film. The oTb doped PCBM as the electron transporting layer can significantly enhances the FF of planar inverted perovskite solar cells. For the cells without PEIE layer between the PCBM electron transporting layer and Ag electrode layer, the oTb doping could remove the S-shape in the J-V characteristics with a FF increase from 0.57 to 0.73. For the cells with PEIE coating, the oTb doping increase the FF from 0.70 to 0.82. These results show the potential of the antibiotic and antimicrobial compound of oTb in the applications of solution-processed electronics.

Author contributions R. G., F. Q. and Y. H. Z. conceived the idea. R. G. and F. Q. performed the solar cell fabrication, optimization and measurement. R. G., F. Q. and S. X. X. performed the film conductivity measurement. Y. H. Z. directed this work. R. G. wrote the first draft of the manuscript. All the authors revised and approved the manuscript.

Fig. 5 Time-resolved photoluminescence (PL) decay of glass/ MAPbI$_3$/(oTb)PCBM with different doping ratios

References

1. http://www.nrel.gov/ncpv/images/efficiency_chart.jpg

2. Polman A, Knight M, Garnett E C, Ehrler B, Sinke W C. Photovoltaic materials: present efficiencies and future challenges. Science, 2016, 352(6283): aad4424

3. Correa-Baena J P, Saliba M, Buonassisi T, Grätzel M, Abate A, Tress W, Hagfeldt A. Promises and challenges of perovskite solar cells. Science, 2017, 358(6364): 739–744

4. Rajagopal A, Yao K, Jen A K. Toward perovskite solar cell commercialization: a perspective and research roadmap based on interfacial engineering. Advanced Materials, 2018, 30(32):

e1800455

5. Jiang Y, Luo B, Jiang F, Jiang F, Fuentes-Hernandez C, Liu T, Mao L, Xiong S, Li Z, Wang T, Kippelen B, Zhou Y. Efficient colorful perovskite solar cells using a top polymer electrode simultaneously as spectrally selective antireflection coating. Nano Letters, 2016, 16 (12): 7829–7835

6. Qin F, Tong J H, Ge R, Luo B W, Jiang F Y, Liu T F, Jiang Y Y, Xu Z Y, Mao L, Meng W, Xiong S X, Li Z F, Li L Q, Zhou Y H. Indium tin oxide (ITO)-free, top-illuminated, flexible perovskite solar cells. Journal of Materials Chemistry A, Materials for Energy and Sustainability, 2016, 4(36): 14017–14024

7. Bai Y, Meng X, Yang S. Interface engineering for highly efficient and stable planar p-i-n perovskite solar cells. Advanced Energy Materials, 2018, 8(5): 1701883

8. Luo D, Yang W, Wang Z, Sadhanala A, Hu Q, Su R, Shivanna R, Trindade G F, Watts J F, Xu Z, Liu T, Chen K, Ye F, Wu P, Zhao L, Wu J, Tu Y, Zhang Y, Yang X, Zhang W, Friend R H, Gong Q, Snaith H J, Zhu R. Enhanced photovoltage for inverted planar heterojunction perovskite solar cells. Science, 2018, 360(6396): 1442–1446

9. Gu P Y, Wang N, Wang C Y, Zhou Y C, Long G K, Tian M M, Chen W Q, Sun X W, Kanatzidis M G, Zhang Q C. Pushing up the efficiency of planar perovskite solar cells to 18.2% with organic small molecules as the electron transport layer. Journal of Materials Chemistry A, Materials for Energy and Sustainability, 2017, 5(16): 7339–7344

10. Li M, Zhao C, Wang Z K, Zhang C C, Lee H K K, Pockett A, Barbé J, Tsoi W C, Yang Y G, Carnie M J, Gao X Y, Yang W X, Durrant J R, Liao L S, Jain S M. Interface modification by ionic liquid: a promising candidate for indoor light harvesting and stability improvement of planar perovskite solar cells. Advanced Energy Materials, 2018, 8(24): 1801509

11. Mali S S, Hong C K. p-i-n/n-i-p type planar hybrid structure of highly efficient perovskite solar cells towards improved air stability: synthetic strategies and the role of p-type hole transport layer (HTL) and n-type electron transport layer (ETL) metal oxides. Nanoscale, 2016, 8(20): 10528–10540

12. Wang Z K, Liao L S. Doped charge-transporting layers in planar perovskite solar cells. Advanced Optical Materials, 2018, 6(17): 1800276

13. Zhao T, Chueh C C, Chen Q, Rajagopal A, Jen A K Y. Defect passivation of organic–inorganic hybrid perovskites by diammonium iodide toward high-performance photovoltaic devices. ACS Energy Letters, 2016, 1(4): 757–763

14. Liang P W, Chueh C C, Williams S T, Jen A K Y. Roles of fullerene-based interlayers in enhancing the performance of organometal perovskite thin-film solar cells. Advanced Energy Materials, 2015, 5 (10): 1402321

15. Kuang C, Tang G, Jiu T, Yang H, Liu H, Li B, Luo W, Li X, Zhang W, Lu F, Fang J, Li Y. Highly efficient electron transport obtained by doping PCBM with graphdiyne in planar-heterojunction perovskite solar cells. Nano Letters, 2015, 15(4): 2756–2762

16. Tang C G, Ang M C, Choo K K, Keerthi V, Tan J K, Syafiqah M N, Kugler T, Burroughes J H, Png R Q, Chua L L, Ho P K. Doped polymer semiconductors with ultrahigh and ultralow work functions for ohmic contacts. Nature, 2016, 539(7630): 536–540

17. Chang C Y, Huang W K, Chang Y C, Lee K T, Chen C T. A solution-processed n-doped fullerene cathode interfacial layer for efficient and stable large-area perovskite solar cells. Journal of Materials Chemistry A, Materials for Energy and Sustainability, 2016, 4(2): 640–648

18. Zhou H, Chen Q, Li G, Luo S, Song T B, Duan H S, Hong Z, You J, Liu Y, Yang Y. Interface engineering of highly efficient perovskite solar cells. Science, 2014, 345(6196): 542–546

19. Yuan D X, Yuan X D, Xu Q Y, Xu M F, Shi X B, Wang Z K, Liao L S. A solution-processed bathocuproine cathode interfacial layer for high-performance bromine-iodine perovskite solar cells. Physical Chemistry Chemical Physics, 2015, 17(40): 26653–26658

20. Lin Y, Shen L, Dai J, Deng Y, Wu Y, Bai Y, Zheng X, Wang J, Fang Y, Wei H, Ma W, Zeng X C, Zhan X, Huang J. π-conjugated lewis base: efficient trap-passivation and charge-extraction for hybrid perovskite solar cells. Advanced Materials, 2017, 29(7): 1604545

21. Hu L, Liu T, Sun L, Xiong S, Qin F, Jiang X, Jiang Y, Zhou Y. Suppressing generation of iodine impurity via an amidine additive in perovskite solar cells. Chemical Communications, 2018, 54(37): 4704–4707

22. Jiang Y Y, Li J, Xiong S X, Jiang F Y, Liu T F, Qin F, Hu L, Zhou Y H. Dual functions of interface passivation and n-doping using 2,6-dimethoxypyridine for enhanced reproducibility and performance of planar perovskite solar cells. Journal of Materials Chemistry A, Materials for Energy and Sustainability, 2017, 5(33): 17632–17639

23. Ye Q Q, Wang Z K, Li M, Zhang C C, Hu K H, Liao L S. N-type doping of fullerenes for planar perovskite solar cells. ACS Energy Letters, 2018, 3(4): 875–882

24. Li M, Wang Z K, Kang T, Yang Y, Gao X, Hsu C S, Li Y, Liao L S. Graphdiyne-modified cross-linkable fullerene as an efficient electron-transporting layer in organometal halide perovskite solar cells. Nano Energy, 2018, 43: 47–54

25. Hu L, Liu T, Duan J, Ma X, Ge C, Jiang Y, Qin F, Xiong S, Jiang F, Hu B, Gao X, Yi Y, Zhou Y. An amidine-type n-dopant for solution-processed field-effect transistors and perovskite solar cells. Advanced Functional Materials, 2017, 27(41): 1703254

26. Bin Z Y, Li J W, Wang L D, Duan L. Efficient n-type dopants with extremely low doping ratios for high performance inverted perovskite solar cells. Energy & Environmental Science, 2016, 9 (11): 3424–3428

27. Wang Z, McMeekin D P, Sakai N, van Reenen S, Wojciechowski K, Patel J B, Johnston M B, Snaith H J. Efficient and air-stable mixed-cation lead mixed-halide perovskite solar cells with n-doped organic electron extraction layers. Advanced Materials, 2017, 29(5): 1604186

28. Beaula T J, Muthuraja P, Sethuram M, Dhandapani M, Rastogi V K, Jothy V B. Biological and spectral studies of O-tolyl biguanide: experimental and theoretical approach. Journal of Molecular Structure, 2017, 1128: 290–299

29. Zhou Y, Fuentes-Hernandez C, Shim J, Meyer J, Giordano A J, Li H, Winget P, Papadopoulos T, Cheun H, Kim J, Fenoll M, Dindar A, Haske W, Najafabadi E, Khan T M, Sojoudi H, Barlow S, Graham S, Brédas J L, Marder S R, Kahn A, Kippelen B. A universal method to produce low-work function electrodes for organic electronics. Science, 2012, 336(6079): 327–332

30. Jiang F Y, Liu T F, Luo B W, Tong J H, Qin F, Xiong S X, Li Z F,

Zhou Y H. A two-terminal perovskite/perovskite tandem solar cell. Journal of Materials Chemistry A, Materials for Energy and Sustainability, 2016, 4(4): 1208–1213

31. Liu T, Jiang F, Qin F, Meng W, Jiang Y, Xiong S, Tong J, Li Z, Liu Y, Zhou Y. Nonreduction-active hole-transporting layers enhancing open-circuit voltage and efficiency of planar perovskite solar cells. ACS Applied Materials & Interfaces, 2016, 8(49): 33899–33906

Ru Ge received her B.S. degree from Huazhong University of Science and Technology (HUST) in 2016. She is now a M.S. student in Wuhan National Laboratory for Optoelectronics, HUST, Wuhan. Her current research interests focus on conducting polymers and interface engineering in organic photovoltaics.

Fei Qin received his B.S. degree from Huazhong University of Science and Technology (HUST) in 2015. He is now a Ph.D. candidate in Wuhan National Laboratory for Optoelectronics, HUST, Wuhan. His Ph.D. research includes interface engineering and flexible, stretchable solar cells.

Lin Hu received his B.S. (2013) and M.S. (2016) degrees at Nanchang University, China. He is currently pursuing his Ph.D. under the supervision of Prof. Yinhua Zhou in Wuhan National Laboratory for Optoelectronics, Huazhong University of Science and Technology, Wuhan. His current research interests focus on materials development and device engineering in organic and perovskite solar cells.

Sixing Xiong received his B.S. degree from Huazhong University of Science and Technology in 2014. He is now a Ph.D. candidate in Wuhan National Laboratory for Optoelectronics, Huazhong University of Science and Technology, Wuhan. His research includes device engineering in flexible solar cells and printed electronics.

Prof. **Yinhua Zhou** received his bachelor (2003) and Ph.D. (2008) degrees both from Jilin University, China. During his Ph.D. study, he spent one year in Prof. Olle Inganäs group as a visiting Ph.D. student in 2007–2008. After that, he worked as postdoctoral fellow in the Georgia Institute of Technology from 2009 to 2013 with Prof. Bernard Kippelen. Since October of 2013, he started the current position as a faculty member in Wuhan National Laboratory for Optoelectronics, Huazhong University of Science and Technology. His research interest includes conducting polymers, organic photovoltaics and printed electronics.